ORIGINAL PAPER

Multi-dimensional MR spectroscopy: towards a better understanding of hepatic encephalopathy

**Manoj K. Sarma · Amir Huda · Rajakumar Nagarajan · Charles H. Hinkin ·
Neil Wilson · Rakesh K. Gupta · Enrique Frias-Martinez · James Sayre · Barry Guze ·
Steven-Huy Han · M. Albert Thomas**

Abstract Hepatic encephalopathy (HE) is normally diagnosed by neuropsychological (NP) tests. The goals of this study were to quantify cerebral metabolites, separate glutamate (Glu) from glutamine (Gln) in patients with minimal hepatic encephalopathy (MHE) as well as healthy subjects using the prior-knowledge fitting (ProFit) algorithm on data acquired by two-dimensional (2D) localized correlated spectroscopy (L-COSY) on two different MR scanners, and to correlate the metabolite changes with neuropsychological (NP) tests. We studied 14 MHE patients and 18 healthy controls using a GE 1.5 T Signa MR scanner. Another group of 16 MHE patients and 18 healthy controls were studied using a Siemens 1.5 T Avanto MR scanner. The following parameters were used for L-COSY: TR/TE=2 s/30 ms, $3\times3\times3$ cm^3 voxel size, 96 Δt_1 increments with 8 averages per Δt_1. Using the ProFit algorithm, we were able to differentiate Gln from Glu on the GE 1.5 T data in the medial frontal white/gray matter. The ratios of myo-inositol (mI), Glu, total choline, scyllo-inositol (sI), phosphoethanolamine (PE), and total N-acetyl aspartate (NAA) showed statistically significant decline in HE patients compared to healthy controls, while the ratio of Gln was significantly increased. Similar trend was seen in the ProFit quantified Siemens 1.5 T data in the frontal and occipito-parietal white/gray regions. Among the NP domain scores, motor function, cognitive speed, executive function and the global scores showed significant differences. Excellent correlations between various NP domains and metabolite ratios were also observed. ProFit based cerebral metabolite quantitation enhances the understanding and basis of the current hypothesis of MHE.

Keywords MRS · COSY · Hepatic encephalopathy · Glutamine · Glutamate · Neuropsychological tests

M. K. Sarma · A. Huda · R. Nagarajan · N. Wilson ·
E. Frias-Martinez · J. Sayre · M. A. Thomas (✉)
Department of Radiological Sciences,
David Geffen School of Medicine, University of California,
CHS BL 428, 10833 Le Conte Avenue,
Los Angeles, CA 90095–1721, USA
e-mail: athomas@mednet.ucla.edu

A. Huda
Department of Physics, California State University,
Fresno, CA, USA

C. H. Hinkin · B. Guze · M. A. Thomas
Department of Psychiatry, David Geffen School of Medicine,
University of California,
Los Angeles, CA, USA

C. H. Hinkin
VA Greater Los Angeles Healthcare System,
Los Angeles, CA, USA

R. K. Gupta
Department of Radiology, Sanjay Gandhi Post-Graduate Institute
of Medical Sciences,
Lucknow, India

S.-H. Han
Department of Hepatology, David Geffen School of Medicine,
University of California,
Los Angeles, CA, USA

Introduction

Hepatic encephalopathy (HE) is a complex neuropsychiatric disorder that complicates acute and chronic liver failure. HE encompasses a wide spectrum of neuropsychiatric abnormalities and motor disturbances that range from mild cognitive impairment to coma and death (Mullen 2007; Wang 2004; Ferenci et al. 2002; McPhail and Taylor-Robinson 2010). It

occurs in two distinct forms: acute, that results from the rapid onset of severe inflammatory and necrotic liver disease, and the more common form, chronic, which is associated with liver failure and slowly evolving neurological features that manifest over time. Acute HE results in movement disorder and impaired consciousness which may progress to coma and severe neurological dysfunction in the syndrome's most severe form (Gitlin 1996; Bernthal et al. 1987), whereas chronic HE describes the neuropsychiatric syndrome, most commonly associated with hepatic dysfunction and portosystemic shunting in cirrhosis. This may also exist in patients with surgical portosystemic shunts (McPhail and Taylor-Robinson 2010). In most patients, the condition is "minimal", and over the past few decades, the focus has shifted to this subgroup of patients who show no gross clinical symptoms of brain dysfunction but who perform poorly on psychometric tests when compared to other patients with cirrhosis and healthy controls (Butterworth 2000; Butterworth 1995; Gilberstadt et al. 1980; Schomerus et al. 1981; Tarter et al. 1984; McCrea et al. 1996). These patients are labeled as having minimal hepatic encephalopathy (MHE) (Ferenci et al. 2002; Schomerus and Hamster 1998; Lockwood 2000; Weissenborn et al. 2001). MHE may be found in 20% to 60% of patients with cirrhosis (Amodio et al. 2004; Dhiman and Chawla 2009; Amodio et al. 2010) depending on the tests used for diagnosis and the severity of hepatic failure. MHE is discernible in prolongation of reaction times in the activities of daily living, such as driving and operating machinery. It has a prognostic value in relation to occurrence of both bouts of acute HE (Saxena et al. 2002; Romero-Gómez 2007; Amodio et al. 2001; Amodio et al. 1999) and death (Amodio et al. 2001; Romero-Gómez et al. 2007).

Conventionally, MHE patients are identified on the basis of a battery of neuropsychological (NP) tests (Butterworth 1995; Blei and Cordoba 1996; Chalasani and Gitlin 1997; Fraser and Arieff 1985; Ross et al. 1996). They show deficiencies in tests of psychomotor speed, concentration, visual attention, tracking, and visuospatial and fine motor skills, while appearing normal on standard bedside neurological examinations (Ferenci et al. 2002; Blei and Cordoba 1996; Duyn et al. 1993). However, the results of these tests are not very specific and do not reveal the underlying neurochemical pathophysiology (Ferenci et al. 2002; Amodio et al. 2004; Binesh et al. 2006). Furthermore, these tests can be subject to confounding factors such as age, superimposed mood disorders, and educational effects (Stewart and Smith 2007). Therefore, there has been increasing interest in the use of noninvasive imaging techniques, such as magnetic resonance imaging (MRI) and magnetic resonance spectroscopy (MRS), to assist in the evaluation of MHE (Foerster et al. 2009). These methods may complement the NP examination.

In particular, MRS has been used extensively as a noninvasive tool to examine the role of cerebral metabolites *in vivo* for the diagnosis of both clinical (acute) and MHE. As reported by Ross et al (Ross et al. 1996; Kreis et al. 1992; Ross et al. 1994), proton (^{1}H) MRS of brain white matter in patients with HE demonstrated a triad of changes in cerebral metabolites: a significant decrease in the myoinositol (mI), a small decline in choline (Cho), and an elevation in the glutamate/glutamine (Glx) concentration with respect to creatine (Cr). Studies have indicated that MRS can detect MHE with a sensitivity approaching 90% (Ross et al. 1994). One-dimensional (1D) MRS, used in these studies, suffers from the severe spectral overlap of various metabolites resonating within a limited spectral range, leading to varying phase artifacts with echo time (TE), which may result in inaccurate quantification for many metabolites. Further, some low concentration metabolites are also not detectable. Two-dimensional (2D) MRS conquers this difficulty by adding a second frequency dimension to each spectrum by acquiring multiple 1D free induction decays (FID) with incrementally longer TEs and applying a 2D Fourier transform on the set of spectra to produce a 2D spectrum (Thomas et al. 2001). By applying a localized two-dimensional correlated spectroscopic (2D L-COSY) sequence on a conventional 1.5 T scanner in healthy human brains, Thomas et al. (Thomas et al. 2001) showed that in addition to detecting N-acetyl aspartate (NAA), Glx, Cho, Cr, and mI, several J-coupled multiplets of metabolites such as aspartate (Asp), phosphocholine (PCh), threonine (Thr), phosphoethanolamine (PE), γ-aminobutyric acid (GABA), and taurine (Tau) can also be identified. Some of these metabolites, such as Asp and Tau, have been directly implicated in the pathogenesis of HE (Hilgier et al. 2000; Lavoie et al. 1987; Butterworth 1996). Binesh et al. (2005) and Singhal et al. (2010) showed that the 2D L-COSY sequence can be applied successfully to MHE patients. They confirmed the earlier findings of 1D MRS studies in MHE and showed that additional metabolites can be detected. Their results showed a statistically significant decrease of mI and Cho, and an increase of Glx in patients when compared to healthy controls. In addition, Binesh et al. (2005) also found an increased Tau in MHE patients.

In the previous studies, changes of Glx have been reported instead of Glu and Gln separately. Attempts in the past have focused on resolving glutamine from glutamate using high field MRS (9.4 T) data processed by LC-Model (Provencher 1993). However no reports of resolving these metabolites at 1.5 T MRS have been published. Although the cross peaks of Glx are much better separated from other overlapping metabolites in 2D L-COSY, glutamate could still not be separated from glutamine because of the almost identical peak locations. In this work we adapt the prior-knowledge fitting (ProFit) (Schulte and Boesiger 2006;

Frias-Martinez et al. 2008) procedure for L-COSY spectroscopy and show that via 2D prior knowledge fitting, glutamate and glutamine can be separately quantified with reasonable precision. In contrast to methods based on simple line fitting and peak integration, commonly applied for metabolite quantification in 2D MRS of brain, ProFit yields metabolite concentration ratios that are independent of sequence and field strength. It fits COSY spectra as linear combinations of 2D basis spectra using a nonlinear least-squares algorithm in combination with a linear least-squares algorithm and incorporates maximum prior knowledge available. In summary, the goals of this study were 1) to quantify cerebral metabolites in MHE patients and healthy subjects using the Profit algorithm to the 2D L-COSY data acquired on 1.5 T MR scanners manufactured by two different vendors, thereby providing further support for the use of MR spectroscopy in clinical research, 2) to separate glutamate and glutamine using Profit and investigate the results in understanding of MHE and 3) to correlate the metabolite changes with NP tests.

Materials and methods

A. Human subjects

14 patients with MHE (53.3 ± 10.6 years) and 18 control subjects (52.7 ± 12.6 years) were studied with a 1.5 T GE MR scanner (GE Medical Systems, Waukesha, WI, USA) between 2000 and 2004. Also, 16 MHE patients (49.6 ± 14.7 years) and 18 control (50.1 ± 10.8 years) subjects were studied with a 1.5 T Siemens Avanto MR scanner (Siemens Medical Solutions, Erlangen, Germany) between 2004 and 2008. We used inclusion criteria of being listed for organ liver transplantation (OLT) and having a United Network Organ Sharing (UNOS) status of 3 or greater. The exclusion criteria included a lack of fluency in the English language (affecting psychometric tests), claustrophobia during MR examination, age less than 18 or more than 75 years, active alcoholism during the past 3 months, HE grades II–IV, gastrointestinal bleeding or infection during the past week, and any brain shunt procedures before the study. The Institutional Review Board (IRB) approved the protocol, and informed consent was obtained from each human subject prior to study participation.

B. MRS Acquisition and Post-processing

A body coil "transmission" and a 3 inch surface coil "reception" were used for the GE scanner. Before applying the L-COSY sequence, a three dimensional (3D) localizer scan followed by a high resolution T_1-weighted axial scan (TR/TE=800/8 ms, 35 slices, 4 mm thickness with no gap) were collected. We used CHESS (Haase et al. 1985) sequence on the GE scanner for water suppression. 2D L-COSY spectra were recorded using the following parameters: TE=30 ms, TR=2000 ms, total number of scans=768 (96 Δt_1 increments and 8 averages per Δt_1), and spectral width F_1=625 Hz and F_2=2500 Hz. A 27 mL voxel was placed on the anterior cingulate gyrus [38] since the NP tests have indicated an alteration predominantly in the frontal tasks that require attention and mental flexibility. The total duration for each 2D scan was approximately 25 min. The voxel shim and suppression were done manually, and a line width of 7–8 Hz was achieved.

For the Siemens Avanto MR scanner, high resolution T_1-weighted images were collected using a magnetization prepared rapid acquisition gradient echo (MPRAGE) pulse sequence (TR=1660 ms; TE=3.87 ms; inversion time=900 ms; FA=10°; matrix size=256×256; FOV=230×230 mm^2; slice thickness=1.2 mm; number of slices=176). A quadrature body coil for "transmission" and a dual surface coil for "reception" were used for the MRS study. One of the surface coils was placed on the right forehead and the other one on the left occipital region of the subject. L-COSY was performed over two locations: prefrontal dorsolateral white/gray matter and occipito-parietal white/gray matter (Singhal et al. 2010) with a 27 mL voxel used for volume localization. A WET-based sequence was used for global water suppression (Ogg et al. 1994) and spectra were recorded using the following parameters: TR=2000 ms, TE=30 ms, total number of scans=768, scan time=25 min (96 Δt_1 increments and 8 averages per Δt_1), spectral width F_1=625 Hz and F_2=2000 Hz. A line width of 8–10 Hz was achieved by manual shimming in all the subjects,

For both GE and Siemens data analysis, 2D L-COSY spectra were processed using the Profit algorithm. Before Fourier transformation, all matrices were filtered via a skewed squared-sine bell function, and then zero-filled in both dimensions to 2048 by 256. Prior to fitting, frequency shifts in F_1 and F_2 as well as zeroth-order phase correction were applied to the L-COSY spectra. The basis spectra used for fitting were simulated numerically with the GAMMA (general approach to magnetic resonance mathematical analysis) library (Smith et al. 1994), using previously reported chemical shifts and coupling constants from the literature (Govindaraju et al. 2000). A set of 19 basis metabolites turned out to be the most suitable choice for fitting L-COSY HE spectra acquired in vivo: Cr, Glu, Gln, NAA, N-acetyl-aspartylglutamate (NAAG), mI, Cho, scyllo-inositol (sI), alanine (Ala), Tau, Asp, glycerylphosphocholine (GPC), PCh, PE, glutathione (GSH), GABA, lactate (Lac), glucose (Glc), and ascorbic acid (Asc). No absolute quantification was attempted, but metabolite concentrations were determined as ratios to Cr. Using the known concentration of Cr, these results can be converted to millimolar concentration or institutional units after application of the requisite correction factors.

C. NP Tests

Neuropsychological testing was conducted by a clinical psychologist on the same day as the MRS scan on those subjects studied by Siemens 1.5 T MR scanner and took approximately 2 h to complete. For better evaluation of the results, the tests were classified into domains according to the ability they tested (Lezak 1995). The domains with the respective NP tests are: 1) Premorbid Estimate of Verbal Intelligence (Wechsler test of adult reading), 2) Learning and Memory (revised Hopkins verbal learning test and revised brief visuospatial memory test), 3) Cognitive Speed/Speed of Information Processing (WAIS-III Digit Symbol, WAIS-III Symbol Search and Trail Making test Part A), 4) Abstraction/Executive Functioning (Wisconsin Card Sorting test (64-item version), Trail Making test Part B and Stroop Color Word test), 5) Attention/Working Memory (Continuous Performance test-II, Paced Auditory Serial Addition Task-50 and WAIS-III Letter-Number Sequencing), 6) Visuospatial Function (WAIS-III Block Design), 7) Motor (Grooved Pegboard (Dominant and Nondominant)), 8) Language (Letter Fluency test (FAS)), 9) Psychiatric Status (Brief Symptom Inventory and Beck Depression Inventory-II) (Lezak 1995). The raw scores for the individual tests were converted to demographically corrected t-scores using published normative data (Heaton et al. 1991). Domain t-scores were calculated by averaging the t-score of the individual tests comprising the neuro-cognitive domain. A Global t-score was then obtained by averaging the individual test scores.

D. Statistical Analysis

All data analysis was performed using SPSS 18.0 for Windows (SPSS Inc., Chicago, IL). The mean and standard deviation (SD) of metabolite concentration ratios with respect to Cr were calculated for MHE patients and healthy controls. To statistically evaluate the hypothesis that there is no difference in the metabolite concentrations ratios between the population groups, a two-tailed t-test and a one-way analysis of variance (ANOVA) were performed. Metabolite concentration ratio differences with p value less than 0.05 were considered to be statistically significant. To explore for any relationship between the metabolite concentration ratios and the NP t-scores, Pearson correlation was performed on the patient data. A Bonferroni-like adjustment (Larzelere and Mulak 1977) was used so that all correlations were still significant with the adjusted alpha level. A logistic regression analysis (Hilbe 2009; Hosmer and Lemeshow 1995) was performed on all the modalities and their combinations to compare their predictability in correctly classifying the patients and healthy controls. Variables were selected with the same $p<0.05$ significant level.

Results

GE 1.5 T

Figure 1(a) shows the 2D contour plots of a L-COSY spectrum acquired using the GE 1.5 T from a voxel size of 27 mL in the medial frontal gray/white matter region of a 35 year old healthy volunteer (top). The middle spectrum is the fitted one using ProFit and the bottom one is the residual difference. The combined prior knowledge 2D spectrum simulated using a GAMMA library is shown in Fig. 1(b). The ProFit quantified metabolite ratios (mean ± SD) of MHE patients and healthy controls acquired from the GE 1.5 T scanner are given in Table 1. The ratios of mI, Glu, total choline (GPC + PCh + Cho), sI, PE, and total NAA showed significant decline in patients compared to healthy controls, whereas the ratio of Gln was significantly increased. For a better visualization of the fluctuation of metabolite ratios among patients and their respective differences with healthy controls, bar graphs were plotted
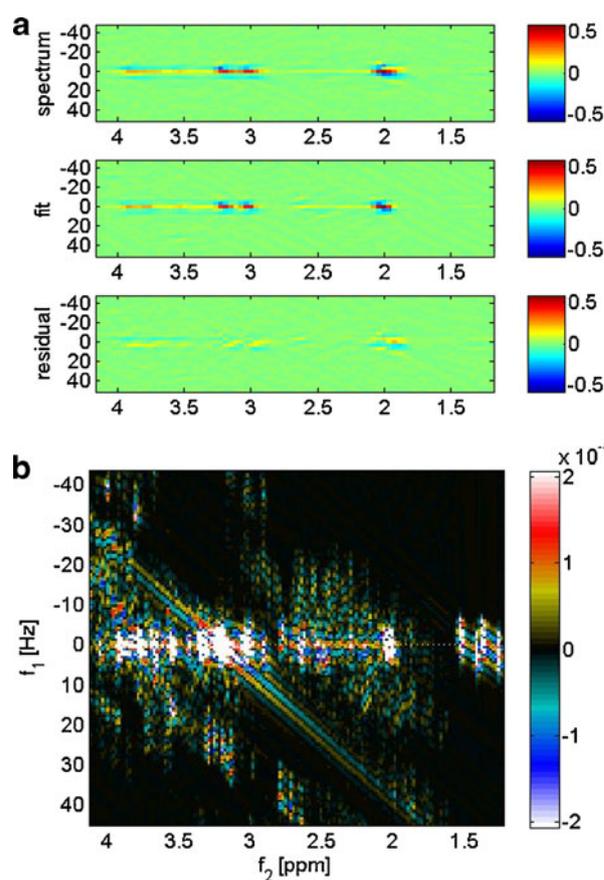
Fig. 1 **a.** A ProFit-processed 2D L-COSY spectrum recorded from the medial frontal white/gray matter of a 35-year-old healthy subject. The abscissae and the ordinates represent f2[ppm] and f1[Hz], respectively. **b.** 2D spectra of the basis set of metabolites used in ProFit processing. The 2D spectra are presented as logarithmically-scaled color plots

Table 1 Metabolite ratios (Mean ± SD) calculated from MHE and healthy subjects in the medial frontal region for the GE 1.5 T acquired COSY data

Metabolites	Controls (mean ± SD)	Patients (mean ± SD)	p-value
Gln	0.227±0.054	0.521±0.186	<0.001[**]
Glu	1.279±0.140	1.098±0.190	0.006[**]
mI	0.690±0.073	0.437±0.099	<0.001[**]
Cho	0.294±0.119	0.277±0.092	0.656
GPC	0.214±0.080	0.161±0.096	0.131
sI	0.067±0.030	0.042±0.018	0.011[**]
PE	0.044±0.010	0.034±0.011	0.040[**]
Tau	0.109±0.044	0.163±0.087	0.079
Glc	0.276±0.129	0.300±0.149	0.644
GSH	0.129±0.109	0.157±0.112	0.511
Ala	0.044±0.023	0.066±0.049	0.147
Asp	0.042±0.024	0.073±0.036	0.111
NAA	0.814±0.223	0.698±0.157	0.101
NAAG	0.398±0.080	0.352±0.088	0.144
Glu + Gln	1.506±0.156	1.618±0.318	0.246
GPC + PCh + Cho	0.521±0.058	0.448±0.076	0.007[**]
NAA ± NAAG	1.212±0.210	1.050±0.186	0.030[**]

** Significant at the 0.05 level

for the major metabolites that showed significant differences between healthy controls and patients as presented in Fig. 2(a) and (b).

Siemens 1.5 T

Figure 3(a) shows the ratios of Gln, Glu, mI, and total choline with respect to Cr, calculated from the ProFit processing of the Siemens 1.5 T 2D L-COSY spectra acquired in the frontal white/gray matter region of MHE patients and healthy subjects. These results were in excellent agreement with the Profit quantitation of GE 1.5 T data as shown in Table 1 and Fig. 2(a). Figure 3(b) shows selected metabolite ratios quantified by the ProFit algorithm in the occipito-parietal region. The findings in the frontal white/gray region were in general agreement with the occipito-parietal region, namely, significantly lowered mI, Glu, and total choline and significantly increased Gln ratios compared to healthy controls.

NP Tests

The NP test results are summarized in Table 2. Significant differences were found between the patients and healthy volunteers in the following domains: motor function, cognitive speed, executive function, and the global scores ($p<0.05$). In patients, the lowest average scores were found in the motor and the cognitive speed domain (<40). Tables 3 and 4 show the significant correlation between various NP domains score and the MRS indices from the Siemens 1.5 T acquired data in the frontal white and occipito-parietal regions respectively. Frontal and occipito-parietal mI ratios

positively correlated with motor and cognitive speed domain scores. Frontal mI ratios additionally correlated with global and visuospatial scores. Also in the frontal region, Gln correlated with global score, Tau with attention, sI with motor and total choline with language and attention. In the occipito-parietal region, total choline, total NAA, and Glx correlated with visuospatial and PE with cognitive speed and global scores.

Logistic regression analysis

The results of logistic regression analysis are shown in Fig. 4. Among the frontal MRS ratios, mI gave the best predictability. The mI and Gln ratios were the only significant variables in the occipito-parietal lobe. Out of the NP tests, cognitive speed and memory were the selected domains. On combining NP tests and MRS ratios, the selected variables were motor and frontal lobe mI and had a predictability of 100%.

Discussion

The current study attempts to separate Glu from Gln, quantify several cerebral metabolites using Profit algorithm and correlate the metabolite changes with NP tests in patients with MHE. Our results demonstrate that Profit fitting of L-COSY data, from both GE and Siemens 1.5 T scanner, was able to quantify Glu and Gln reliably. There are no reports of separating these metabolites while post-processing the 1.5 T and 3 T MRS data. Hence, this finding is first of its kind. The mI ratio was found to be the most

Fig. 2 **a** and **b**. Metabolite ratios from the GE acquired COSY data in the medial frontal gray/white matter region. Only the metabolites that demonstrated significant change in MHE patients are shown
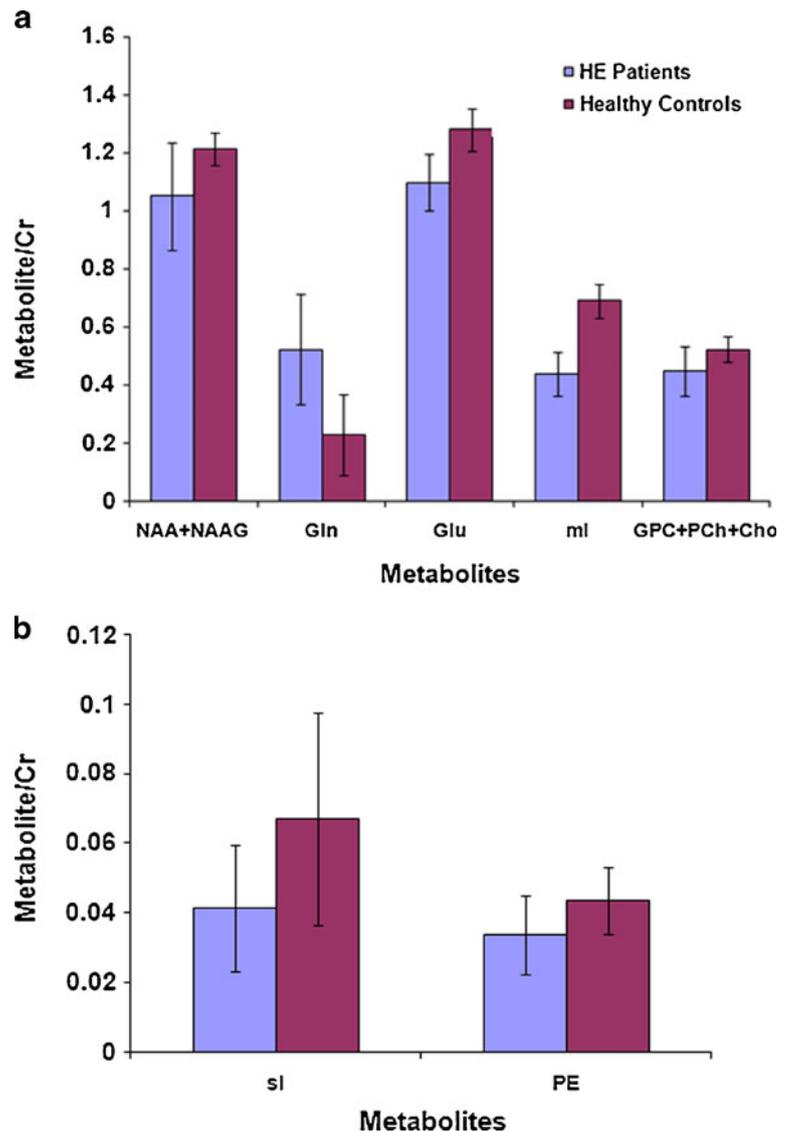
significant variable among other MRS ratios and NP domains. We found significant impairment in cognitive speed, motor function, executive function and global domain scores in the patient group. The strong correlations between the significantly altered MRS ratios and NP domains imply that the metabolite ratio changes not only are clinically relevant but also may be responsible for the neuropsychological manifestations.

Following is a brief discussion of each metabolite demonstrating significant difference in MHE patients via Profit processing of L-COSY, its putative role in the brain, and possible implication in hepatic encephalopathy. We discuss each metabolite, if and how, multidimensional MRS datasets acquired on the GE and Siemens 1.5 T MR scanners, add to the basis of our understanding of the pathogenesis of MHE.

Neuronal activity triggers various responses that act together to adapt and deliver the energy substrates for local

neuronal needs. The neuronal activity is determined primarily by electric (rate of action potential firing) and synaptic activity. Glu released from glutamatergic synapses is taken up by the astrocytes in cotransport with sodium, thereby increasing intracellular sodium and stimulating the sodium-potassium pump (Pellerin and Magistretti 1997), which increases the astrocytic adenosine-triphosphate (ATP) consumption, and hence links the astrocytic glucose metabolism to neuronal glutamate release (Magistretti et al. 1999). Since the blood-brain barrier is quite impermeable to Glu, almost all brain Glu is synthesized from Glc, Gln, or from the degradation of proteins (Gruetter et al. 1994).

It is generally understood that in MHE, the increased brain concentration of ammonia is correlated with increased permeability of the blood-brain barrier (BBB) to ammonia (Lockwood et al. 1991a) and the increase of Gln in astrocytes since ammonia is metabolized via glutamine

Fig. 3 Metabolite ratios from the Siemens acquired COSY data in: **a.** the frontal white/gray and **b.** occipito-parietal white/gray regions. Only the metabolites that demonstrated significant change in MHE patients are shown
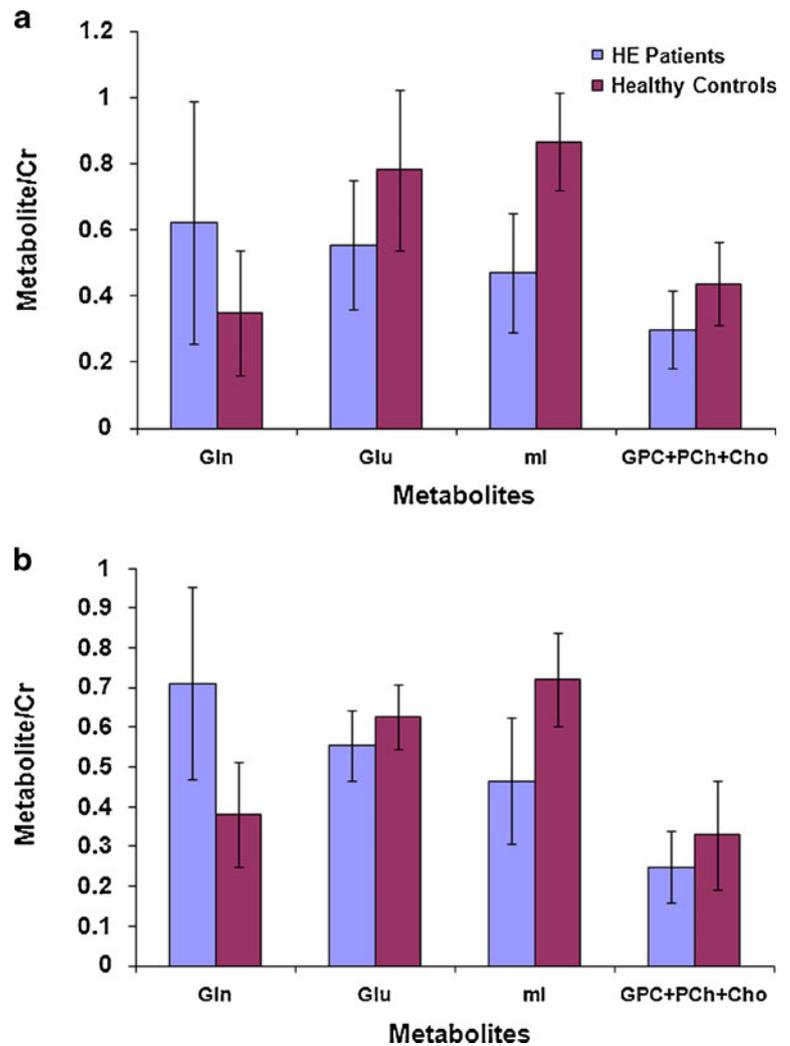
synthetase (GS) mediated amidation of Glu into Gln (Berl et al. 1962). This increase of Gln could contribute to the decrease of total brain concentration of Glu in hyperammonemia long known in rats with acute hyperammonemia of acute liver failure (ALF) induced by thioacetamide (Bosman et al. 1990). Decreased Glu has also been seen in patients with cirrhosis who died in hepatic coma (Lavoie et al. 1987).

However, in 1D proton MRS, it is very difficult to separate the resonances of Glu from Gln and quite often the two are reported together as Glx. Thus, the increase of Gln is quite often foreshadowed by the decrease in Glu and the total peak of Glx is reported as an increase. With the ProFit algorithm used in 2D proton MRS, we clearly see a significant decrease in Glu and an increase in Gln as shown in Table 1 and in keeping with the ammonia detoxification hypothesis. Reduc-

Table 2 The mean t-scores of the individual NP domains relevant to the Siemens acquired L-COSY data

NP Domains	Healthy Controls (mean ± SD)	Patients (mean ± SD)	p-value
Visuospatial	42.01±06.49	40.19±08.53	0.541
Language	46.50±11.08	39.79±07.40	0.072
Motor	43.96±11.67	33.78±11.78	0.033[**]
*CogSpeed	47.71±09.66	36.46±06.77	0.002[**]
Attention	42.82±04.22	44.25±07.05	0.533
*Exec	50.38±06.69	42.67±09.20	0.020[**]
Memory	46.64±10.68	41.93±07.05	0.185
Global	45.80±04.07	40.69±05.10	0.008[**]

*Exec, executive function; CogSpeed, cognitive speed.

** Significant at the 0.05 level

Table 3 Pearson Correlation between the frontal MRS ratios and NP domain scores in MHE patients for the Siemens acquired L-COSY data

Frontal	NP domain	Correlation Coefficients	p-value
Gln	Language	−0.5	0.098
	Global	−0.634	0.027**
Glu	Attention	0.777	0.069
	Executive	−0.765	0.076
mI	Visuospatial	0.604	0.049**
	Motor	0.719	0.013**
	CogSpeed	0.603	0.05**
	Global	0.665	0.025**
GPC+PCh+Cho	Language	0.743	0.009**
	Attention	0.613*	0.045**
Tau	Attention	−0.771	0.005**
sI	Motor	−0.951	0.049**
Glx	Visuospatial	−0.549	0.064
	Global	−0.533	0.074

** Significant at the 0.05 level

tion in Glu could also be partly due to reduced synthesis from Glc and the influence of ammonia on Glu pools other than the astrocytes (Zwingmann et al. 2003).

Several lines of evidence have also shown that increased ammonia exposure can lead to decreased uptake of Glu by the astrocytes (Vaquero and Butterworth 2006). This could lead to reduced local Glc oxidation. In addition, astrocyte swelling (discussed later) is an important feature of both acute and chronic liver failure and this can potentially lead to a change in transport processes.

Cho is important for normal membrane function, lipid transport, and methyl metabolism. It is a precursor of betaine, used by the kidney to maintain water balance and by the liver as a source of methyl groups for methionine formation (Koc et al. 2002). In the central nervous system, it is an important precursor of choline-containing membrane phospholipids such as phosphatidylcholine (PtdCho)

and sphingomyelin in neurons and glial cells and of acetylcholine (ACho) in cholinergic neurons.

The pool of total choline in the rat brain is large; however, 90% of the total choline is bound in the phospholipids of the cell membranes such as PtdCho and a further 9% in hydrophilic metabolites such as PCh and GPC. Similarly in the rat blood plasma, 99% of total choline is present in choline-containing phospholipids, and only 1% is present as free and the hydrophilic choline metabolites (Klein et al. 1993). Free choline, in contrast to other choline-containing metabolites, is the only well-defined pathway for choline supply from the blood into the brain. There is no data indicating major transport of choline-containing phospholipids into and out of the brain under physiological conditions (Pardridge et al. 1979).

In an *in vivo* proton MRS correlation study of the Cho peak with *in vitro* chemical measures of choline-containing

Table 4 Pearson Correlation between the occipito-parietal MRS ratios and NP domain scores in MHE patients for the Siemens acquired L-COSY data

Occipital	NP domain	Correlation Coefficients	p-value
Gln	Motor	−0.658	0.054
	CogSpeed	−0.638	0.065
mI	Motor	0.675	0.023**
	CogSpeed	0.772	0.005**
GPC+PCh+Cho	Visuospatial	0.585	0.036**
PE	Visuospatial	0.68	0.093
	CogSpeed	0.886	0.008**
	Global	0.814	0.026**
sI	Visuospatial	0.781	0.067
NAA+NAAG	Visuospatial	0.709	0.01**
	Executive	0.56	0.058
	Global	0.543	0.068
Glx	Visuospatial	−0.627	0.039**
	Global	−0.525	0.098

** Significant at the 0.05 level
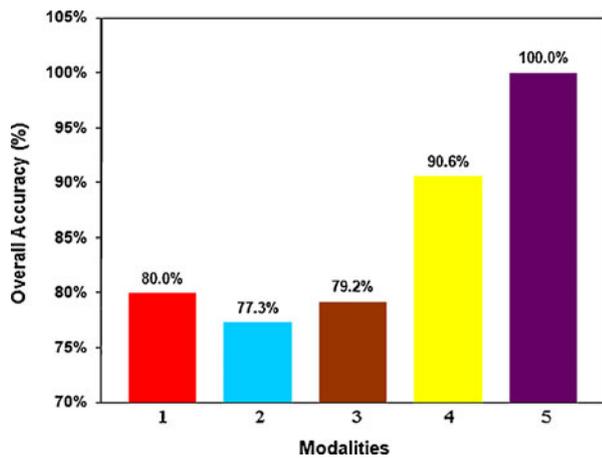
Fig. 4 Logistic Regression Analysis results: 1- occipito-parietal MRS (mI), 2- occipito-parietal MRS (Gln), 3-frontal MRS (mI), 4-NP (cognitive speed + motor), 5-NP (motor), and frontal MRS (mI)

compounds, the proton MRS Cho peak strongly correlated with free Cho and hydrophilic metabolites such as PCh (membrane synthesis) and to some extent with GPC (membrane degradation) but not with membrane-bound, PtdCho (Miller et al. 1996).

Unfortunately, 1D proton MRS *in vivo* techniques cannot differentiate the trimethyl protons of choline from those of PCh and GPC as their signals are separated by less than 0.03 ppm (Loening et al. 2005). The ^{31}P resonances of PCh and GPC, on the other hand, differ from one another by ~3.5 ppm and can be used for better quantification (Bhujwalla et al. 1999). However, the improved sensitivity of ^{1}H nuclei for detection, makes a strong case for using proton MRS. 2D proton MRS with ProFit algorithm enables separation for GPC and the total choline peaks.

In human cerebral neoplasms, it has been shown both *in vivo* and *in vitro* via ^{31}P MRS that the phospholipid composition of cell membranes is changed (Kaibara et al. 1998). This change in phospholipid metabolism is seen in two resonances: the phosphomonoester (PME) and the phosphodiester (PDE) (Griffiths et al. 1983). The aqueous extracts of a tissue, when analyzed *in vitro* by high resolution ^{31}P MRS, can show the two phospholipid precursors, PCh and PE in the PME signal while the PDE signal includes the degradation products GPC and glycer-ophosphoethanolamine (GPE) (Evanochko et al. 1984). In tumors, the PME resonance has been found to be increased, a change explained by an accumulation of PCh and PE (Solivera et al. 2009).

In HE, the typical ^{31}P MR spectrum contains resonances assigned to PME, inorganic phosphate (Pi), PDE, phospho-creatine, γATP, αATP, and βATP, all providing information on energy metabolism. However, no single consensus has emerged from these studies although Taylor-Robinson group has consistently demonstrated reduction in PME

and PDE to βATP ratio (Taylor-Robinson et al. 1994; Taylor-Robinson et al. 1999; Patel et al. 2000).

Our 2D proton MRS results show a pattern similar to that observed by the Taylor-Robinson group, i.e., a reduction in GPC (although not reaching significance perhaps, due to high standard deviation) as well as a significant decline in total choline including free choline, PCh and GPC in patients when compared to healthy controls (see Table 1). In addition, a significant decline is also observed in PE, clearly pointing to a decrease in the phospholipid metabolism in MHE. This is a new insight not decipherable solely from the data in 1D proton MRS and points to the need for techniques such as 2D proton MRS to tease out these inferences.

mI is an organic osmolyte presumed to serve as a compensatory tool of astrocytes to buffer ammonia-induced increase in glutamine within the astrocytes, which can lead to swelling. The swelling can have implications on trans-porters such as Glu. However, effective compensation shift takes time for astrocyte volume homeostasis. ALF as opposed to chronic liver failure happens too rapidly to allow this compensatory shift and hence, mI/Cr ratio is not significantly different in patients with ALF compared to the healthy controls. Since the application of MRS in MHE, it has been shown in 1D MRS that mI concentration is significantly reduced in patients to maintain the astrocytic volume. With the application of 2D MRS, we were able to verify this finding as well as significant reduction of a similar osmolyte, sI belonging to the inositol group in these patients.

GSH is a primary antioxidant and plays an important role in oxidative stress protection in living cells. GSH is a tripeptide, consisting of glycine, cysteine, and glutamate. GSH is quite difficult to observe via 1D proton MRS even though its concentration is not very low (~1-3 mM) because of severe overlap with much more intense signals of creatine, glutamate, and aspartate. 2D proton MRS can clearly delineate GSH and with the ProFit algorithm, we have been able to quantify its concentration. Studies of GSH levels in blood and urine, have shown that subjects with risk factors of stroke have relatively low levels of GSH and patients with acute ischemic stroke develop elevated blood levels of GSH during the first hours to days post ictus (Zimmerman et al. 2004).

In our study of MHE, we found a general trend towards increase of GSH in patients compared to controls. However, the changes were found to be non-significant possibly due to technical difficulties at 1.5 T. In liver dysfunction, like in stroke, time may be of significance in how the cells cope with stress and what the resultant systemic consequence may be in acute and chronic cases. Hence, it would be quite useful to employ 2D proton MRS in cases of ALF to see the levels of GSH and compare it with our findings.

Tau is another metabolite not observable via 1D proton MRS. It is one of the most abundant free amino acids in the brain and is localized in both neuronal and glial compartments. Autopsied brain tissue from patients who died of hepatic coma has shown significantly decreased Tau in the prefrontal cortex (Butterworth 1996). Opposite to this, our results show an increasing trend in Tau in patients with MHE compared to healthy controls using both GE and Siemens 1.5 T MRS data. The biochemical significance of this finding is unclear. It is unknown if the subjects considered in the autopsied results were in the early stages (MHE) or late stages of HE. At the same time, in our L-COSY study, the 2D cross peak of Tau occurs very close to the diagonal and as a result could be effected by line-width changes from a patient to another. To understand all these changes, a more detailed study is required.

Glc is the major energy substrate for the brain that is degraded by glycolysis, the tricarboxylic acid (TCA) cycle, and oxidative phosphorylation (Chih and Roberts 2003). Neuronal activity and local Glc use and consumption are strongly correlated with the local blood flow (Clarke and Sokoloff 1999). Brain Glc transport involves the breaching of two barriers: the BBB formed by the capillary endothelial cells, which are effectively connected together by tight junctions, and the barrier formed by the plasma membranes of neurons and astrocytes to which Glc must be delivered. The transport parameters of BBB Glc transport as well as the passage of many other substances including ions and water can be modulated by various extracellular and intracellular messengers, and also by pathologic stimuli involving metabolic, osmotic, or oxidative stress (Leybaert 2005).

In MHE, Lockwood et al. have reported via positron emission tomography (PET) that for whole-slice cerebral blood flow (CBF) and cerebral metabolic rate of glucose (CMR_{glc}), the values were not different in this group of patients versus healthy controls. However, for both CBF and CMR_{glc}, there was a highly significant difference in the pattern of flow and metabolism. Higher values for both flow and metabolism were observed in the cerebellum, thalamus, and caudate in patients and lower values in the cortex (Lockwood et al. 1991b). Weissenborn et al. (2007) have also reported via PET both CMR_{glc} and CMR_{NH3} in patients with MHE. They found similar alteration in cerebral glucose utilization as reported by Lockwood et al. (Lockwood et al. 1991b) except for a decrease in glucose metabolism in the motor cortex and stable or increased glucose utilization rate within the frontolateral cortex. When it comes to MRS, again 1D proton MRS is unable to differentiate the resonances of Glc. In our 2D MRS study, in the frontal cortex, we did not observe any significant differences in Glc concentration in the MHE patients compared to the healthy controls.

Conclusions

In summary, we have shown that ProFit-processed 2D L-COSY data demonstrates clear separation of glutamine from glutamate. This differentiation would be quite useful in studying many other diseases and disorders since 1D spectroscopy has been quite limited in its ability to separately quantify these overlapping metabolites. Our results also confirm the earlier findings of 1D MRS studies in MHE and show that additional metabolites that occur at low concentration (≤ 1 mM) can be detected and quantified, shedding light on the underlying mechanisms of the pathogenesis of MHE. The combination of ProFit and multidimensional spectroscopy turns out to be advantageous in quantifying J-coupled metabolites like Asp, PCh, Thr, PE, GABA, and Tau. We have also observed significant correlations between the metabolite ratios calculated from L-COSY and the neurocognitive functions assessed by the NP tests.

References

Amodio P, Del Piccolo F, Marchetti P, Angeli P, Iemmolo R, Caregaro L, Merkel C, Gerunda G, Gatta A (1999) Clinical features and survival of cirrhotic patients with subclinical cognitive alterations detected by the number connection test and computerized psychometric tests. Hepatology 29:1662–1667

Amodio P, Del Piccolo F, Pettenò E, Mapelli D, Angeli P, Iemmolo R, Muraca M, Musto C, Gerunda G, Rizzo C, Merkel C, Gatta A (2001) Prevalence and prognostic value of quantified electroencephalogram (EEG) alterations in cirrhotic patients. J Hepatol 35:37–45

Amodio P, Montagnese S, Gatta A, Morgan MY (2004) Characteristics of minimal hepatic encephalopathy. Metab Brain Dis 19:253–267

Amodio P, Ridola L, Schiff S, Montagnese S, Pasquale C, Nardelli S, Pentassuglio I, Trezza M, Marzano C, Flaiban C, Angeli P, Cona G, Bisiacchi P, Gatta A, Riggio O (2010) Improving detection of minimal hepatic encephalopathy using the inhibitory control task. Gastroenterology 139:510–518

Berl S, Tokagaki G, Clarke DD, Waelsch H (1962) Metabolic compartments in vivo. Ammonia and glutamic acid metabolism in brain and liver. J Biol Chem 237:2562–2569

Bernthal P, Hayes A, Tarter RE, Van Thiel D, Lecky J, Hegedus A (1987) Cerebral CT scan abnormalities in cholestatic and hepatocellular disease and their relationship to neuropsychologic test performance. Hepatology 7:107–114

Bhujwalla ZM, Aboagye EO, Gillies RJ, Chacko VP, Mendola CE, Backer JM (1999) Nm23-transfected MDA-MB-435 human breast carcinoma cells form tumors with altered phospholipid metabolism and pH: a ^{31}P nuclear magnetic resonance study *in vivo* and *in vitro*. Magn Reson Med 41:897–903

Binesh N, Huda A, Bugbee M, Gupta R, Rasgon N, Kumar A, Green M, Han S, Thomas MA (2005) Adding another spectral dimension to ^{1}H magnetic resonance spectroscopy of hepatic encephalopathy. J Magn Reson Imaging 21:398–405

Binesh N, Huda A, Thomas MA, Wyckoff N, Bugbee M, Han S, Rasgon N, Davanzo P, Sayre J, Guze B, Martin P, Fawzy F (2006) Hepatic encephalopathy: a neurochemical, neuroanatomical, and neuropsychological study. J Appl Clin Med Phys 7:86–96

Blei AT, Cordoba J (1996) Subclinical encephalopathy. Digest Dis 14:2–11

Bosman DK, Deutz NE, De Graaf AA, vd Hulst RW, Van Eijk HM, Bovée WM, Maas MA, Jörning GG, Chamuleau RA (1990) Changes in brain metabolism during hyperammonemia and acute liver failure: results of a comparative 1H-NMR spectroscopy and biochemical investigation. Hepatology 12:281–290

Butterworth RF (1995) Hepatic encephalopathy. Neurologist 1:95–104

Butterworth RF (1996) Taurine in hepatic encephalopathy. Adv Exp Med Biol 403:601–606

Butterworth RF (2000) Complication of cirrhosis. III. Hepatic encephalopathy. J Hepatol 32:171–180

Chalasani N, Gitlin N (1997) Subclinical hepatic encephalopathy: How best to diagnose? Am J Gastroent 92:905–906

Chih CP, Roberts EL Jr (2003) Energy substrates for neurons during neural activity: a critical review of the astrocyte-neuron lactate shuttle hypothesis. J Cereb Blood Flow Metab 23:1263–1281

Clarke DD, Sokoloff L (1999) Circulation and energy metabolism of the brain. In: Siegel GJ, Agranoff BW et al (eds) Basic neurochemistry. Lippincott-Raven, Philadelphia, pp 637–669

Dhiman RK, Chawla YK (2009) Minimal hepatic encephalopathy. Indian J Gastroenterol 28:5–16

Duyn JH, Gillen J, Sobering G, van Zijl PC, Moonen CTW (1993) Multisection proton MR spectrosocpic imaging of the brain. Radiology 188:277–282

Evanochko WT, Sakal TT, Ng TC, Krishnaa NR, Kimc HD, Zeidlerc RB, Ghantad VK, Brockmane RW, Schifferf LM, Braunschweigerf PG, Glicksona JD (1984) NMR study of in vivo RIF-1 tumors. Analysis of perchloric acid extracts and identification of ^{1}H, ^{31}P and ^{13}C resonances. Biochim Biophys Acta 805:104–116

Ferenci P, Lockwood A, Mullen K, Tarter R, Weissenborn K, Blei AT (2002) Hepatic encephalopathy–definition, nomenclature, diagnosis, and quantification: final report of the working party at the 11th World Congresses of Gastroenterology, Vienna, 1998. Hepatology 35:716–721

Foerster BR, Conklin LS, Petrou M, Barker PB, Schwarz KB (2009) Minimal hepatic encephalopathy in children: evaluation with proton MR spectroscopy. AJNR Am J Neuroradiol 30:1610–1613

Fraser CL, Arieff AI (1985) Hepatic encephalopathy. New Eng J Med 313:865–873

Frias-Martinez E, Rajakumar N, Liu X, Singhal A, Banakar S, Lipnick S, Verma G, Ramadan S, Kumar A, Thomas MA (2008) ProFit-based Quantitation of Cerebral Metabolites using 2D L-COSY at 3 T Magnetic Resonance. Proc Intl Soc Mag Reson Med 16: 691, Toronto, Canada

Gilberstadt SJ, Gilberstadt H, Zieve L, Buegel B, Collier RO Jr, McClain CJ (1980) Psychomotor performance defects in cirrhotic patients without overt encephalopathy. Arch Intern Med 140:519–521

Gitlin N (1996) Hepatic encephalopathy. In: Zorkin D, Boyer TD (eds) Hepatology. Saunders, Philadelphia, pp 605–617

Govindaraju V, Young K, Maudsley AA (2000) Proton NMR chemical shifts and coupling constants for brain metabolites. NMR Biomed 13:129–153

Griffiths JR, Cady E, Edwards RHT, McCready VR, Wilkie DR, Wiltshaw E (1983) ^{31}P-NMR studies of a human tumour in situ. Lancet 1:1435–1436

Gruetter R, Novotny EJ, Boulware SD, Mason GF, Rothman DL, Shulman GI, Prichard JW, Shulman RG (1994) Localized 13C NMR spectroscopy in the human brain of amino acid labeling from D-[1-^{13}C]glucose. J Neurochem 63:1377–1385

Haase A, Frahm J, Haenicke W, Matthaei D (1985) 1H NMR chemical-shift selective (CHESS) imaging. Phys Med Biol 30:341–344

Heaton RK, Grant I, Matthews CG (1991) Comprehensive norms for an expanded Halstead-Reitan battery: demographic corrections, research findings, and clinical applications. Psychological Assessment Resources, Odessa

Hilbe JM (2009) Logistic regression models. Chapman & Hall/CRC Press

Hilgier W, Law RO, Zielinska M (2000) Taurine, glutamine, glutamate, and aspartate content and efflux, cell volume of cerebrocortical minislices of rats with hepatic encephalopathy. Adv Exp Med Biol 483:305–312

Hosmer DW, Lemeshow S (1995) Applied Logistic Regression. John Wiley and Sons, Inc Menard, Scott

Kaibara T, Tyson RL, Sutherland GR (1998) Human cerebral neoplasms studied using MR spectroscopy: a review. Biochem Cell Biol 76:477–486

Klein J, Gonzalez R, Koppen A, Loffelholz K (1993) Free choline and choline metabolites in rat brain and body fluids: sensitive determination and implications for choline supply to the brain. Neurochem Int 22:293–300

Koc H, Mar M, Ranasinghe A, Swenberg JA, Zeisel SH (2002) Quantitation of Choline and its Metabolites in Tissues and Foods by Liquid Chromatography/Electrospray Ionization-Isotope Dilution Mass Spectrometry. Analytical Chemistry 74:4734–4740

Kreis R, Ross BD, Farrow NA, Ackerman Z (1992) Metabolic disorders of the brain in chronic hepatic encephalopathy detected with H-1 MR spectroscopy. Radiology 182:19–27

Larzelere RE, Mulak SA (1977) Single-sample tests for many correlations. Psychol Bull 84:557–569

Lavoie J, Giguere JF, Layrargues GP, Butterworth RF (1987) Amino acid changes in autopsied brain tissue from cirrhotic patients with hepatic encephalopathy. J Neurochem 49:692–697

Leybaert L (2005) Neurobarrier coupling in the brain: a partner of neurovascular and neurometabolic coupling? J Cereb Blood Flow Metab 25:2–16

Lezak MD (1995) Neuropsychological assessment. Oxford University Press, New York, pp 333–685

Lockwood AH (2000) "What's in a name?" Improving the care of cirrhotics. J Hepatol 32:859–861

Lockwood AH, Yap EWH, Wong WH (1991a) Cerebral ammonia metabolism in patients with severe liver disease and minimal hepatic encephalopathy. J Cerebral Blood Flow Metabol 11:337–341

Lockwood AH, Yap EWH, Rhodes HM, Wong WH (1991b) Altered cerebral blood flow and glucose metabolism in patients with liver disease and minimal encephalopathy. J Cerebral Blood Flow Metabol 11:331–336

Loening NM, Chamberlin AM, Zepeda AG, Gonzalez RG, Cheng LL (2005) Quantification of phosphocholine and glycerophosphocholine with ^{31}P edited ^{1}H NMR spectroscopy. NMR in Biomedicine 18:413–420

Magistretti PJ, Pellerin L, Rothman DL, Shulman RG (1999) Energy on demand. Science 283:496–497

McCrea M, Cordoba I, Vessey G, Blei AT, Randolph C (1996) Neuropsychological characterization and detection of subclinical hepatic encephalopathy. Arch Neurol 53:758–763

McPhail MJ, Taylor-Robinson SD (2010) The role of magnetic resonance imaging and spectroscopy in hepatic encephalopathy. Metab Brain Dis 25:65–72

Miller BL, Chang L, Booth R, Ernst T, Cornford M, Nikas D, McBride D, Jenden DJ (1996) In Vivo ^{1}H MRS Choline: Correlation with In Vitro Chemistry/Histology. Life Sciences 58:1929–1935

Mullen KD (2007) Review of the final report of the 1998 Working Party on definition, nomenclature and diagnosis of hepatic encephalopathy. Aliment Pharmacol Ther 25:11–16

Ogg RJ, Kingsley PB, Taylor JS (1994) WET, a T1- and B1-insensitive water-suppression method for in vivo localized 1H NMR spectroscopy. J Magn Reson B 104:1–10

Patel N, Forton DM, Coutts GA, Thomas HC, Taylor-Robinson SD (2000) Intracellular pH measurements of the whole head and the basal ganglia in chronic liver disease: a phosphorus-31 MR spectroscopy study. Metab Brain Dis 15:223–240

Pardridge WM, Cornford EM, Braun LD, Oldendorf WH (1979) Transport of choline and choline analogues through the blood-brain barrier. In: Barbeau A, Growdon JH, Wurtman RJ (eds) Nutrition and the Brain. Raven, New York, pp 25–33

Pellerin L, Magistretti PJ (1997) Glutamate uptake stimulates Na$^+$, K$^+$-ATPase activity in astrocytes via activation of a distinct subunit highly sensitive to ouabian. J Neurochem 69:2132–2137

Provencher SW (1993) Estimation of metabolite concentrations from localized in vivo proton NMR spectra. Magn Reson Med 30:672–679

Romero-Gómez M (2007) Critical flicker frequency: it is time to break down barriers surrounding minimal hepatic encephalopathy. J Hepatol 47:10–11

Romero-Gómez M, Córdoba J, Jover R, del Olmo JA, Ramírez M, Rey R, de Madaria E, Montoliu C, Nuñez D, Flavia M, Compañy L, Rodrigo JM, Felipo V (2007) Value of the critical flicker frequency in patients with minimal hepatic encephalopathy. Hepatology 45:879–885

Ross BD, Danielsen ER, Bluml S (1996) Proton magnetic resonance spectroscopy: The new gold standard for diagnosis of clinical and subclinical hepatic encephalopathy? Digest Dis 14:30–39

Ross BD, Jacobson S, Villamil F, Korula J, Kreis R, Ernst T, Shonk T, Moats RA (1994) Subclinical hepatic encephalopathy: proton MR spectroscopic abnormalities. Radiology 193:457–463

Saxena N, Bhatia M, Joshi YK, Garg PK, Dwivedi SN, Tandon RK (2002) Electrophysiological and neuropsychological tests for the diagnosis of subclinical hepatic encephalopathy and prediction of overt encephalopathy. Liver 22:190–197

Schomerus H, Hamster W (1998) Neuropsychological aspects of portalsystemic encephalopathy. Metab Brain Dis 13:361–377

Schomerus H, Hamster W, Blunck H, Reinhard U, Mayer K, Dolle W (1981) Latent portasystemic encephalopathy. I. Nature of cerebral functional defects and their effect on fitness to drive. Dig Dis Sci 26:622–630

Schulte RF, Boesiger P (2006) ProFit: two-dimensional prior-knowledge fitting of J-resolved spectra. NMR Biomed 19:255–263

Singhal A, Nagarajan R, Hinkin CH, Kumar R, Sayre J, Elderkin-Thompson V, Huda A, Gupta RK, Han SH, Thomas MA (2010) Two-dimensional MR spectroscopy of minimal hepatic encephalopathy and neuropsychological correlates in vivo. J Magn Reson Imaging 32:35–43

Smith SA, Levante TO, Meier BH, Ernst RR (1994) Computer-simulations in magnetic-resonance-an object-oriented programming approach. J Magn Reson A 106:75–105

Solivera J, Cerdan S, Pascual JM, Barrios L, Roda JM (2009) Assessment of 31P-NMR analysis of phospholipid profiles for potential differential diagnosis of human cerebral tumors. NMR in Biomedicine 22:663–674

Stewart CA, Smith GE (2007) Minimal hepatic encephalopathy. Nat Clin Pract Gastroenterol Hepatol 4:677–685

Tarter RE, Hegedus AM, Van Thiel DH, Schade RR, Gavaler JS, Starzl TE (1984) Nonalcoholic cirrhosis associated with neuropsychological dysfunction in the absence of overt evidence of hepatic encephalopathy. Gastroenterology 86:1421–1427

Taylor-Robinson SD, Sargentoni J, Mallalieu RJ, Bell JD, Bryant DJ, Coutts GA, Morgan MY (1994) Cerebral phosphorus-31 magnetic resonance spectroscopy in patients with chronic hepatic encephalopathy. Hepatology 20:1173–1178

Taylor-Robinson SD, Buckley C, Changani KK, Hodgson HJ, Bell JD (1999) Cerebral proton and phosphorus-31 magnetic resonance spectroscopy in patients with subclinical hepatic encephalopathy. Liver 19:389–398

Thomas MA, Yue K, Binesh N, Davanzo P, Kumar A, Siegel B, Frye M, Curran J, Lufkin R, Martin P, Guze B (2001) Localized two-dimensional shift correlated MR spectroscopy of human brain. Magn Reson Med 46:58–67

Vaquero J, Butterworth RF (2006) The brain glutamate system in liver failure. J Neurochem 98:661–669

Wang YM (2004) The definition, nomenclature and diagnosis of hepatic encephalopathy. Zhonghua Gan Zang Bing Za Zhi 12:305–306

Weissenborn K, Ahl B, Fischer-Wasels D, van den Hoff J, Hecker H, Burchert W, Köstler H (2007) Correlations between magnetic resonance spectroscopy alterations and cerebral ammonia and glucose metabolism in cirrhotic patients with and without hepatic encephalopathy. Gut 56:1736–1742

Weissenborn K, Ennen JC, Schomerus H, Ruckert N, Hecker H (2001) Neuropsychological characterization of hepatic encephalopathy. J Hepatol 34:768–773

Zimmerman C, Winnefeld K, Streck S, Roskosb M, Haberla RL (2004) Antioxidant status in acute stroke patients and patients at stroke risk. Eur Neurol 51:157–161

Zwingmann C, Chaturet N, Leibiritz D, Butterworth RF (2003) Selective increase of brain lactate synthesis in experimental acute liver failure: results of a [H-C] nuclear magnetic resonance study. Hepatology 37:420–428